China Ocean Engineering, Vol.10, No.4, pp.419 – 432.
China Ocean Press, 1996. Printed in P.R. China.

Generation and Deformation of Solitary Waves

Chou Chung-Ren* **and Shih Ruey-Syan****

Abstract — Base on the Lagrangian description and finite differencing of the time step, the generation, propagation and deformation of solitary waves are simulated numerically by means of boundary element method. An algorithm to generate waves with any prescribed form is also implanted in the scheme, but in this research, solitary waves are studied. The numerical model is first verified by studying the case of a solitary wave impinging against a vertical wall. Time histories of evolution of a soliton running up on a sloping beach, as well as over a submerged obstacle are then presented. Applications to scattering problems due to solitary waves progressing over a slope onto a shelf are also shown.

Key words: *Lagrangian description, solitary wave, boundary element method, time histories*

1. Introduction

Numerical study of long waves in shallow water has become one of the most important investigations that have been developed by many researchers recently. Based on a set of approximate equations for long waves, the transformation of solitary wave progressing over a slope onto a shelf including the scattering problem was first discussed in detail by Madsen and Mei (1969), who compared the numerical results with some experimental data and obtained reasonable agreement. Later, some numerical solutions of a variable-coefficient Korteweg-de Vries equation are derived by Johnson (1972) in an attempt to describe the development of a single solitary wave moving onto a shelf. Ouyama (1985) explored solitary wave set up on slope by boundary element method. Also, with the application of the Lagrange-particle method, an explicit solution of solitary waves propagating over an uneven bottom was then studied by Okamura and Yakuwa (1987). With the boundary element method, Sugino and Tosaka (1990) analyzed the generation, propagation and deformation of a solitary wave in a water tank with a gentle slope by the mixed Eulerian-Lagrangian mehtod. Chou *et al.* (1996) studied the deformation of solitary waves in coastal zones with submerged obstacles by using the boundary element method in the time domain.

In this study, problems associated with the generation and deformation of solitary waves are considered numerically by boundary element method. Based on the Lagrangian description and finite differencing of the time step, a scheme to generate waves with any prescribed form is implanted in the model. The stability of the model is then cross-checked by the constancy of mass and energies. Furthermore, the scattering of a solitary wave due to a shelf is also discussed and compared with the results obtained by Madsen and Mei, and good agreement is found.

2. Theoretical Analysis

As defined in Fig. 1, Cartesian coordinate system is employed, the origin of which is located on the still water surface and the z-axis pointed positively upwards. The flow field is

* Professor, Dept. of Harbor and River Engineering, National Taiwan Ocean University
** Graduate Student, Dept. of Harbor and River Engineering, National Taiwan Ocean University

bounded by a pseudo- wave- generating boundary Γ_1, a free water surface Γ_2 and an impermeable sea bed Γ_3. The fluid within the region is assumed to be inviscid and incompressible, and the flow is irrotational. Fluid motion has a velocity potential $\Phi(x, z; t)$ satisfying the following Laplace equation:

$$\frac{\partial^2 \Phi}{\partial x^2} + \frac{\partial^2 \Phi}{\partial z^2} = 0 . \tag{1}$$

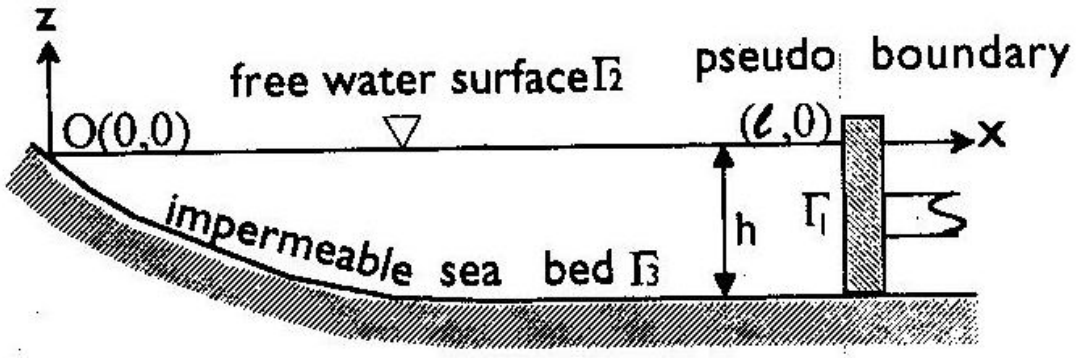

Fig. 1. Definition sketch.

2.1 Boundary Conditions

2.1.1 *Boundary Condition of Pseudo Wave-Making Boundary* Γ_1

The pseudo boundary, Γ_1 is assumed to represent a wave-generating device. Although it is clear that the paddles of any desired type can be simulated, a piston wave generator is assumed for simplicity in this study. Requiring that the horizontal velocities of the pseudo wave-paddle $U(t)$ and fluid flow be continuous, we obtain the following relationship:

$$\bar{\Phi} = \frac{\partial \Phi}{\partial v} = U(t) . \tag{2}$$

Waves can be simulated by selecting suitable input $U(t)$. In this study, solitary waves are simulated, thus $U(t)$ can be expressed as

$$U(t) = x_0 \cdot \omega \cdot \operatorname{sech}^2 [\omega (t - t_c)] \tag{3}$$

$$x_0 = h \sqrt{\frac{4\xi_0}{3(h + \xi_0)}} \tag{4}$$

$$\omega = \sqrt{\frac{g}{h}} \sqrt{\frac{3}{4} \frac{\xi_0}{h} \left(1 + \frac{\xi_0}{h}\right)} \tag{5}$$

$$t_c = \frac{\pi}{\omega} \tag{6}$$

where x_0 denotes the semistroke of the wave-making paddle and ξ_0 is the wave height of solitary wave to be generated.

2.1.2 *Boundary Condition of Free Water Surface*

The atmospheric pressure on the free water surface is assumed to be constant, therefore, the boundary condition can be obtianed from the kinematic and dynamic condition as follows:

$$u = \frac{Dx}{Dt} = \frac{\partial \Phi}{\partial x} \tag{7}$$

$$\omega = \frac{Dz}{Dt} = \frac{\partial \Phi}{\partial z} \tag{8}$$

$$\frac{D\Phi}{Dt} + g\zeta - \frac{1}{2}\left[\left(\frac{\partial \Phi}{\partial x}\right)^2 + \left(\frac{\partial \Phi}{\partial z}\right)^2\right] = 0 \tag{9}$$

where D is the Lagrange differentiation, g is the gravitational acceleration and ζ is the surface elevation.

2.1.3 *Boundary Condition of Impermeable Sea Bed*

From the fact that the water particle velocity normal to the impermeable seabed has to be null, we have

$$\frac{\partial \Phi}{\partial v} = 0 \tag{10}$$

where v is the unit normal vector.

2.2 Integral Equations

According to Green's second identity, velocity potential $\Phi(x, z; t)$ at any point within the region can be expressed using velocity potential on the boundary $\Phi(\xi, \eta; t)$ and its normal derivative $\partial \Phi(\xi, \eta; t) / \partial v$ as

$$\Phi(x, z; t) = \frac{1}{2\pi}\int_\Gamma \left[\frac{\partial \Phi(\xi, \eta; t)}{\partial v} \ln \frac{1}{r} - \Phi(\xi, \eta; t) \frac{\partial}{\partial v} \ln \frac{1}{r}\right] ds \tag{11}$$

where $r = [(\xi - x)^2 + (\eta - z)^2]^{1/2}$.

When the inner point (x, z) approaches the boundary point (ξ', η'), due to its singularity, the velocity potential $\Phi(\xi', \eta'; t)$ can be expressed as

$$\Phi(\xi', \eta'; \ t) = \frac{1}{\pi}\int_{\Gamma}\left[\frac{\partial\Phi(\xi, \eta; \ t)}{\partial v}\ln\frac{1}{R} - \Phi(\xi, \eta; \ t)\frac{\partial}{\partial v}\ln\frac{1}{R}\right] ds \tag{12}$$

where $R = [(\xi - \xi')^2 + (\eta - \eta')^2]^{1/2}$.

In order to proceed with the numerical calculation, the boundaries Γ_1 through Γ_3 are divided into N_1 to N_2 discrete segments respectively with linear elements, and the above equation can then be written in a discretized form as:

$$\Phi_i(\xi', \eta', t) + \frac{1}{\pi}\sum_{j=1}^{N}\int_{\Gamma_j}\left[\Phi_j(\xi, \eta, t)\, M_1 + \Phi_{j+1}(\xi, \eta, t)\, M_2\right]\frac{\partial}{\partial v}\ln\frac{1}{r}\, ds$$

$$= \frac{1}{\pi}\sum_{j=1}^{N}\int_{\Gamma_j}\left[\overline{\Phi}_j(\xi, \eta, t)\, M_1 + \overline{\Phi}_{j+1}(\xi, \eta, t)\, M_2\right]\ln\frac{1}{r}\, ds \tag{13}$$

where $\overline{\Phi}_j = \partial\Phi_j / \partial v$; $\overline{\Phi}_{j+1} = \partial\Phi_{j+1} / \partial v$; M_1, M_2 are the shape functions, $M_1 = (1-\chi)/2$, $M_2 = (1+\chi)/2$; and χ is a local dimensionless coordinate.

Eq. (13) can be expressed in the following matrix form:

$$[\Phi] = [O]\,[\overline{\Phi}] \tag{14}$$

in which $[\Phi]$ and $[\overline{\Phi}]$ are, respectively, the potential function and its normal derivative on the boundaries; and $[O]$ is a matrix related to the geometrical shape of the boundary, where

$$\left.\begin{aligned}
&[\Phi] = \Phi_i, \quad (i = 1 \sim N); \quad [\overline{\Phi}] = \overline{\Phi}_i = \frac{\partial\Phi_i}{\partial v};\\
&[O] = [H + I]^{-1}[G];\\
&[H] = H_{ij}, \quad (i, j = 1 \sim N); \quad [G] = G_{ij}, \quad (i, j = 1 \sim N);\\
&H_{ij} = \begin{cases}\overline{H}_{ij} & (i \neq j)\\ \overline{H}_{ij} + 1 & (i = j)\end{cases}; \quad [I] = \text{unit matrix};\\
&\overline{H}_{ij} = \begin{cases}h^1_{ij} + h^2_{ij-1} & (j \geqslant 2)\\ h^1_{i1} + h^2_{iN} & (j = 1)\end{cases}; \quad G_{ij} = \begin{cases}g^1_{ij} + g^2_{ij-1} & (j \geqslant 2)\\ g^1_{i1} + g^2_{iN} & (j = 1)\end{cases}
\end{aligned}\right\} \tag{15}$$

$$h^1_{ij} = \frac{1}{\pi}\int_{\Gamma_j} M_1 \frac{\partial}{\partial v}\ln\frac{1}{r}\, d\Gamma, \tag{16}$$

$$h^2_{ij} = \frac{1}{\pi}\int_{\Gamma_j} M_2 \frac{\partial}{\partial v}\ln\frac{1}{r}\, d\Gamma, \tag{17}$$

$$g^1_{ij} = \frac{1}{\pi}\int_{\Gamma_j} M_1 \ln\frac{1}{r}\, d\Gamma, \tag{18}$$

$$g^2_{ij} = \frac{1}{\pi}\int_{\Gamma_j} M_2 \ln\frac{1}{r}\, d\Gamma. \tag{19}$$

The numerical scheme has been discussed in detail by Chou (1983).

To facilitate the substitution of the boundary conditions into each boundary, we rewrite Eq. (14) as follows:

$$[\Phi_i] = [O_{ij}][\overline{\Phi}_j], \qquad i, j = 1 \sim 3. \tag{20}$$

2.3 Computational Procedure

2.3.1 *The Initial Conditions*

The initial conditions of each boundary are summarized as follows:

— The pseudo-wave-generating boundary Γ_1

From the requirement of continuity between the horizontal velocity of the pseudo-wave paddle $U(t)$ and the fluid motion, we obtain:

$$\overline{\Phi}_1^0 = \frac{\partial \Phi_1^0}{\partial v} = -U(0) \tag{21}$$

where superscript "0" denotes the beginning time of the simulation.

— The free water surface Γ_2

Assuming that the water surface is initially at rest ($t = 0$), the velocity potential is therefore null, i. e.

$$\Phi_2^0 = 0. \tag{22}$$

— The impermeable sea bed Γ_3

The velocity of fluid particles in the direction normal to the impermeable seabed is null, thus we obtain:

$$\overline{\Phi}_3^0 = \frac{\partial \Phi_3^0}{\partial v} = 0. \tag{23}$$

2.3.2 *The Finite Difference of Related Terms*

The tangential derivative on the free water surface, $(\partial \Phi_2 / \partial s)_i$, can be approximated through the central difference equation:

$$\left.\begin{aligned} \left(\frac{\partial \Phi_2}{\partial s}\right)_i &= \left(\frac{\Delta s_i}{\Delta s_{i+1}}\right) \cdot \frac{\Phi_{2,i+1}}{s'} + (\Delta s_{i+1} - \Delta s_i) \cdot \frac{\Phi_{2,i}}{s''} - \left(\frac{\Delta s_{i+1}}{\Delta s_i}\right) \cdot \frac{\Phi_{2,i-1}}{s'} \\ s' &= \Delta s_{i+1} + \Delta s_i, \qquad s'' = \Delta s_i \cdot \Delta s_{i+1} \\ \Delta s_i &= \sqrt{(\chi_{i+1} - \chi_i)^2 + (Z_{i+1} - Z_i)^2} \end{aligned}\right\} \tag{24}$$

For the free water surface, we have the following relationship:

$$\left.\begin{aligned}\frac{\partial \Phi_2}{\partial x} &= \frac{\partial \Phi_2}{\partial v}\sin\beta - \frac{\partial \Phi_2}{\partial s}\cos\beta \\ \frac{\partial \Phi_2}{\partial z} &= \frac{\partial \Phi_2}{\partial v}\cos\beta + \frac{\partial \Phi_2}{\partial s}\sin\beta\end{aligned}\right\} \tag{25}$$

where β denotes the angle between the tangential direction of the free water surface and the x-axis.

At the k-th time step, the profile of free water surface is expressed by (x^k, z^k) , from Eqs. (7) and (8) the $k+1$-th time step can be expressed by (x^{k+1}, z^{k+1}) step where

$$x^{k+1} = x^k + \left(\frac{\partial \Phi_2^k}{\partial x}\right)\Delta t\,; \tag{26}$$

$$z^{k+1} = z^k + \left(\frac{\partial \Phi_2^k}{\partial z}\right)\Delta t \tag{27}$$

and Δt denotes the discrete time differencing interval.

From Eqs. (9) and (25), the velocity potential of the free water surface at the $k+1$-th time step, Φ^{k+1}, can be approximated through:

$$\Phi_2^{k+1} = \Phi_2^k + \frac{1}{2}\left[\left(\frac{\partial \Phi_2}{\partial s}\right)^2 + \left(\frac{\partial \Phi_2}{\partial v}\right)^2\right]^k \Delta t - g z^{k+1}\Delta t\,. \tag{28}$$

Substituting Eqs. (2), (10) and the above equation into Eq. (20), we can obtain the following simultaneous equations:

$$\begin{bmatrix}\Phi_1 \\ \overline{\Phi}_2 \\ \Phi_3\end{bmatrix}^{k+1} = \begin{bmatrix}I & -O_{12} & 0 \\ 0 & -O_{22} & 0 \\ 0 & -O_{32} & I\end{bmatrix}^{-1}\begin{bmatrix}O_{11} & 0 & O_{13} \\ O_{21} & -I & O_{23} \\ O_{31} & 0 & O_{33}\end{bmatrix}\begin{bmatrix}\overline{\Phi}_1 \\ \Phi_2 \\ \overline{\Phi}_3\end{bmatrix}^{k+1} \tag{29}$$

2.3.3 *The Iterative Scheme*

— By substituting Eqs. (21)~(23) into Eq. (20), the initial values for the normal derivative of the velocity potentials on the water surface, $\partial\,\Phi_2^k / \partial\, v$, the velocity potentials on the pseudo-wave-generator, Φ_1^k, as well as the velocity potentials on the sea bed, Φ_3^k, can be obtained respectively.

— Tangential derivative of velocity potentials on the water surface, $\partial\,\Phi_2^k / \partial\, s$, is then calculated using Eq. (24).

— Surface elevations, (x^{k+1}, z^{k+1}), for the next time step can be obtained from Eqs. (26) and (27).

— The velocity potentials on the free water surface for the next time step are given by Eq. (28).

— At the next time step, $t = k+1\Delta t$, recalculate the coefficients of the matrix $[O]$ in Eq. (20), using the new profiles of the water surface obtained in procedure 3 and the new position of the pseudo wave-paddle.

— Substituting the velocity potentials on the new water surface obtained by procedure 4, the horizontal velocity, $U(t)$, of the pseudo wave paddle given by Eq. (2), and the boundary condition on the sea bed given by substitution of Eq. (10) into Eq. (29), the normal derivative of velocity potentials, $\Phi_2^{k+1} / \partial \nu$, on the water surface, the velocity potentias, Φ_1^{k+1}, on the pseudo wave paddle, and the velocity potentials, Φ_3^{k+1}, on the sea bed, for the time step $t = k+1\Delta t$ can be obtained.

— By repeating procedure 2 through 6, the time history for the generation, propagation and deformation of waves can be simulated.

3. Numerical Results and Discussions

3.1 Time Histories of Wave Profiles

As shown in Fig. 2, the case of soliton propagating against a vertical wall is first considered to verify the present numerical scheme. The incident wave height is $\xi_0 / h = 0.05$. Fig. 3 shows

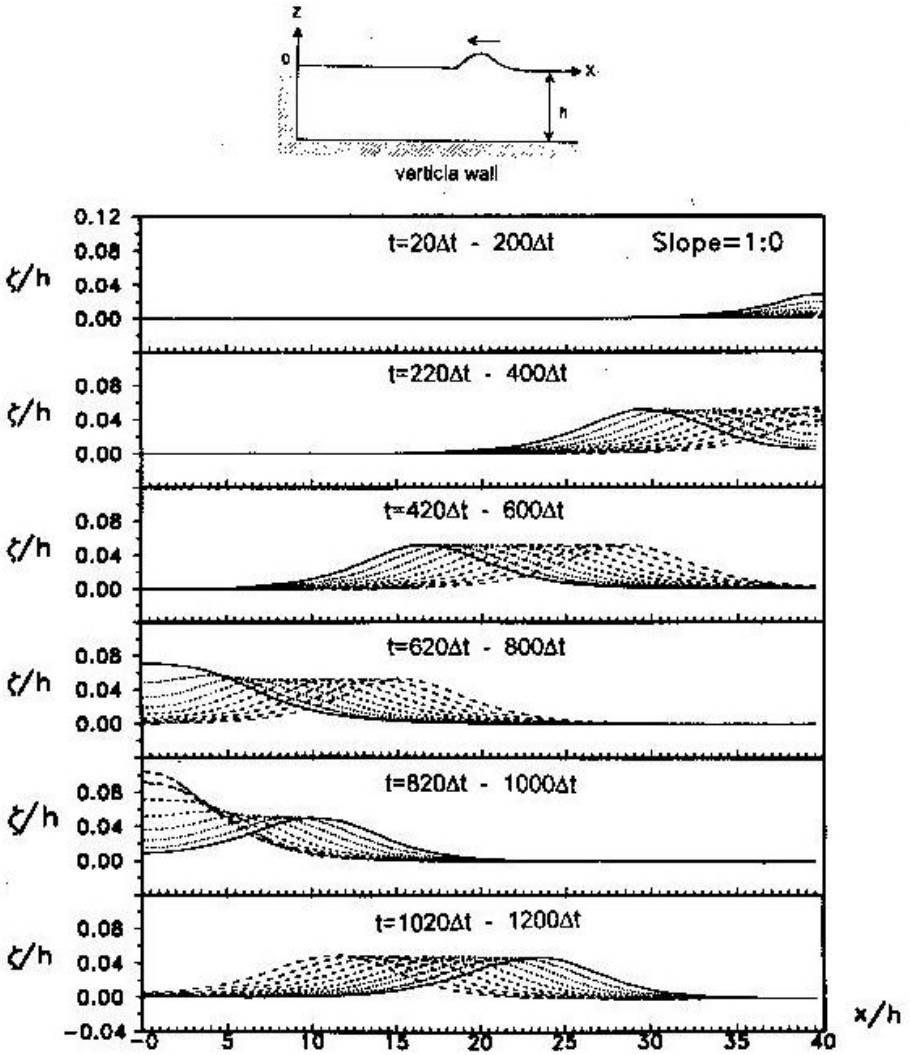

Fig. 2. Time histories of solitary wave propagation and run-up against a vertical wall.
$\xi_0 / h = 0.5$, $t_c = 5.0548$, $\Delta t = t_c / 250$, $\Delta s = L / 40$.

the profile of soliton prior to reflection. A comparison with the theoretical results given by Boussinesq shows good agreement. Fig. 4 shows the time histories of the water surface for various submerged banks fixed in front of the vertical wall, the layout of the bank being given at the top of the figure. Fig. 5 shows the case of an inclined wall with a submerged bank of $d = 0.5$ h in height, the slopes varing from 1:0 to 1:5. The pseudo wave paddle is palced at a distance L_{eff} away from the origin of coordinates, where L_{eff} is the effective wave length of the soliton derived by (Nakayama, 1983):

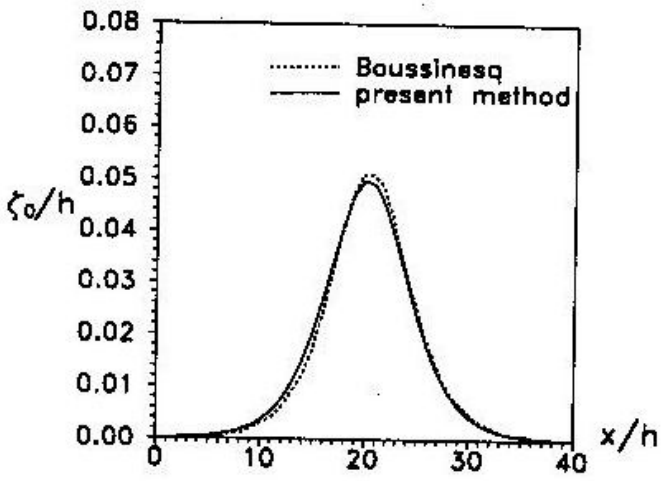

Fig. 3. Comparison of the profiles of solitary wave.

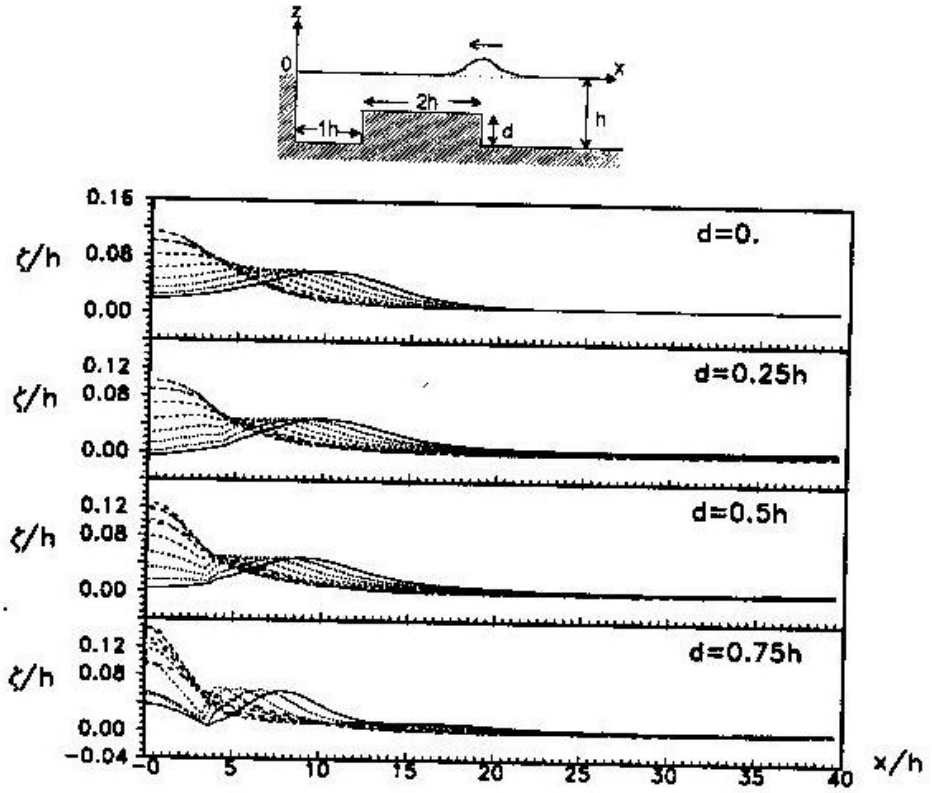

Fig. 4. Time histories of solitary wave propagating and running up on vertical wall with various banks. ($t = 820\,\Delta t \sim 1000\,\Delta t$)

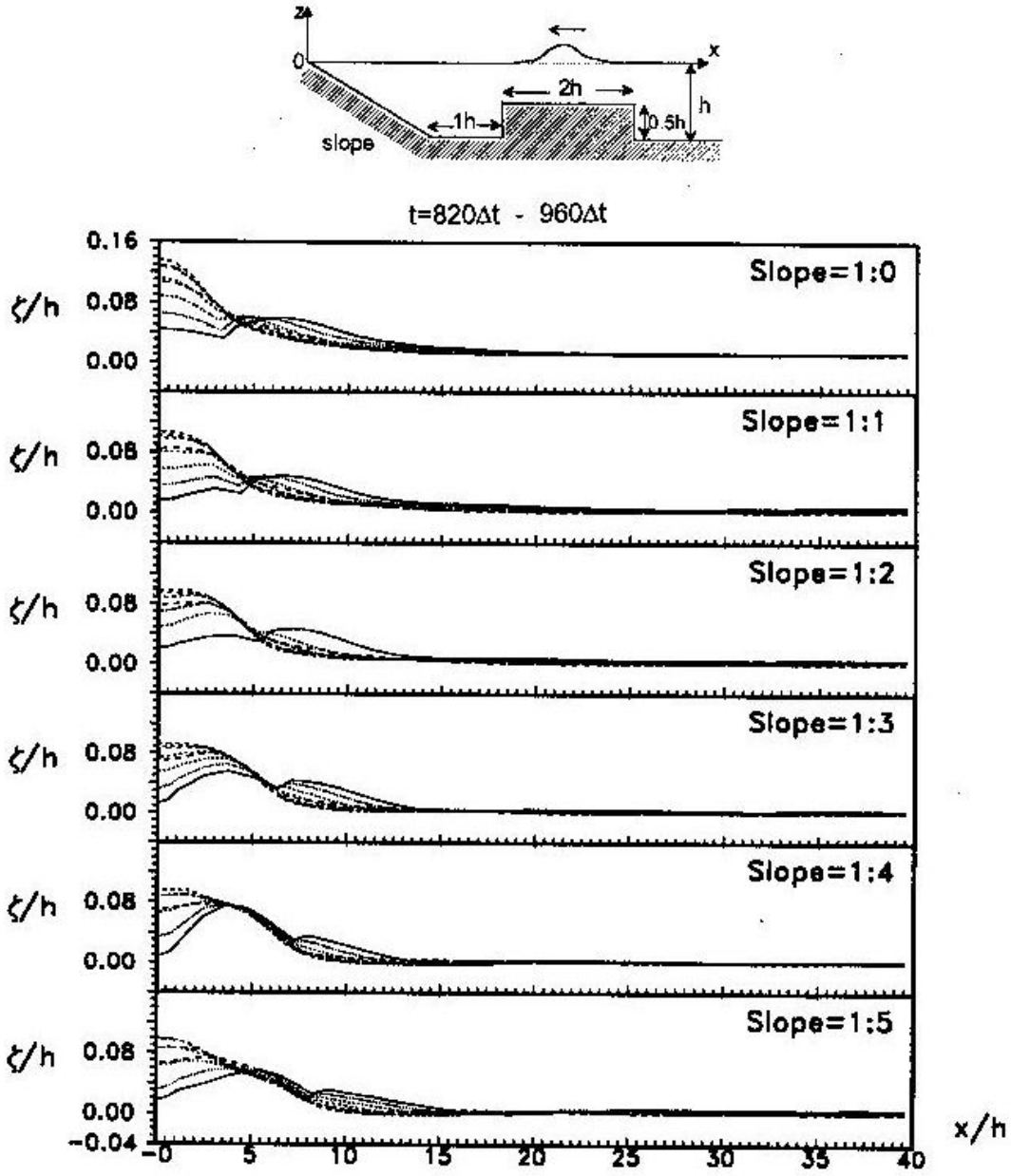

Fig. 5. Profiles of solitary wave on various slopes with submerged bank.

$$L_{\text{eff}} = 9.5766\, h \sqrt{\frac{h}{\xi_0}} \tag{30}$$

In the calculation, the water surface is divided into 40 linear elements, with a discrete time interval of $\Delta t = t_c / 250$.

3.2 Stability Check of the Numerical Model

The conservative property of the present numerical scheme is cross- checked by the continuum equations for mass and energy through the following formula:

$$\left.\begin{aligned} M &= \int_{\Gamma_2} \zeta dx \\ E &= T_e + V \\ T_e &= \frac{1}{2}\int_{\Gamma} \Phi \cdot \overline{\Phi} ds \\ V &= \frac{1}{2} g \int_{\Gamma_2} \zeta^2 dx \end{aligned}\right\} \tag{31}$$

where M denotes the mass of fluid, E is the total energy, and T_e *and* V are the kinetic and potential energy, respectively.

Fig. 6 shows the results for a solitary wave. The mass above the water surface at rest is equal to that of the area the paddle has swept; the total energy is equal to the energy transmitted by the pseudo paddle, and it becomes constant after the piston has stopped. These results are compared with theoretical results:

$$\left.\begin{aligned} M &= 4h^2 \sqrt{\frac{\zeta}{3h}} \\ E &= \frac{3}{8}\rho g h^2 \zeta \sqrt{\frac{\zeta}{3h}} \end{aligned}\right\} \tag{32}$$

From the comparison shown in the figure, it can be found that our results are consistant with theoretical results.

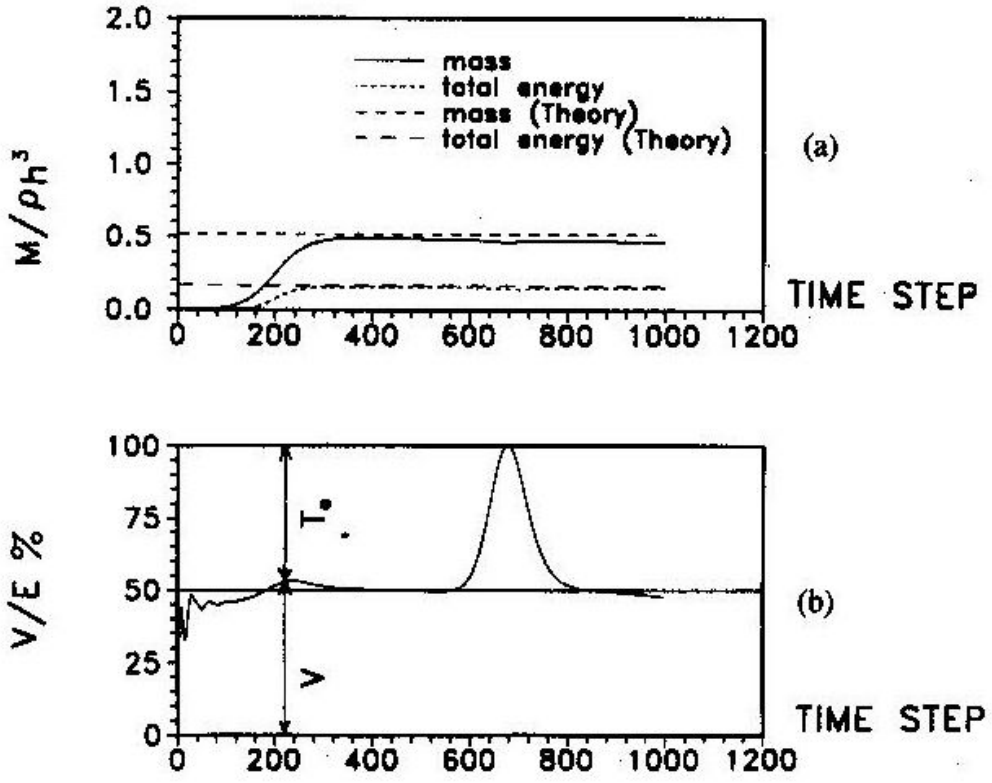

Fig. 6. Variation of mass and energy.
$\zeta_0/h = 0.05$, $t_c = 5.0548$, $t = t_c/200$, $\Delta s = L/40$.

3.3 Scattering of a Solitary Wave

When a solitary wave propagates over a slope onto a shelf, the profile becomes longer peaked as the wave amplitude increases with the distance the wave travels on the shelf, i. e. the larger distance the wave travels on the shelf, the steeper the wave becomes; also, a hump appears at the rear and gradually trails behind the main wave. The deformation of a solitary wave propagating over a slope of 1:20 onto a shelf with a uniform depth of $q = 0.5$ h is shown in Fig. 7(a)~(d), the layout of the shelf being shown at the top of the figure.

The development of wave profile at station A through D is compared with both the theoretial and numerical results obtained by Madsen and Mei (1969), from which it can be found that the results are consistent except for station D, where the wave profile is a little larger. Fig. 8 shows the time histories of a solitary wave propagating over a slope of 1:20 with a shelf of $q =$ 0.5 h, and Fig. 9 shows another case with a slope of 1:30.

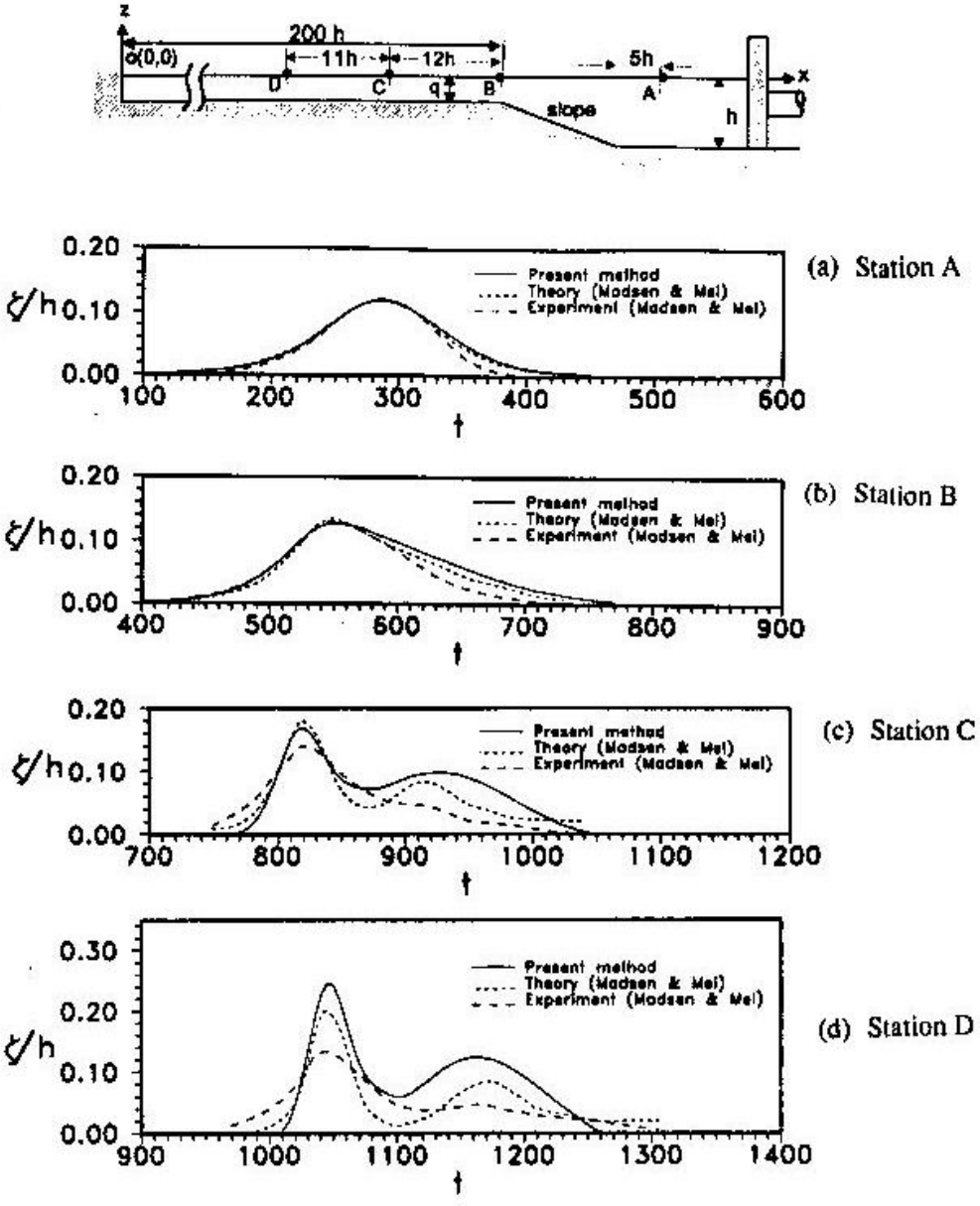

Fig. 7. Deformation of a solitary wave propagating over a slope onto a shelf. $\xi_0 / h = 0.12$, $t_c = 3.1593$, $\Delta t = t_c / 200$, $q / s = 0.5$, slope = 1:20.

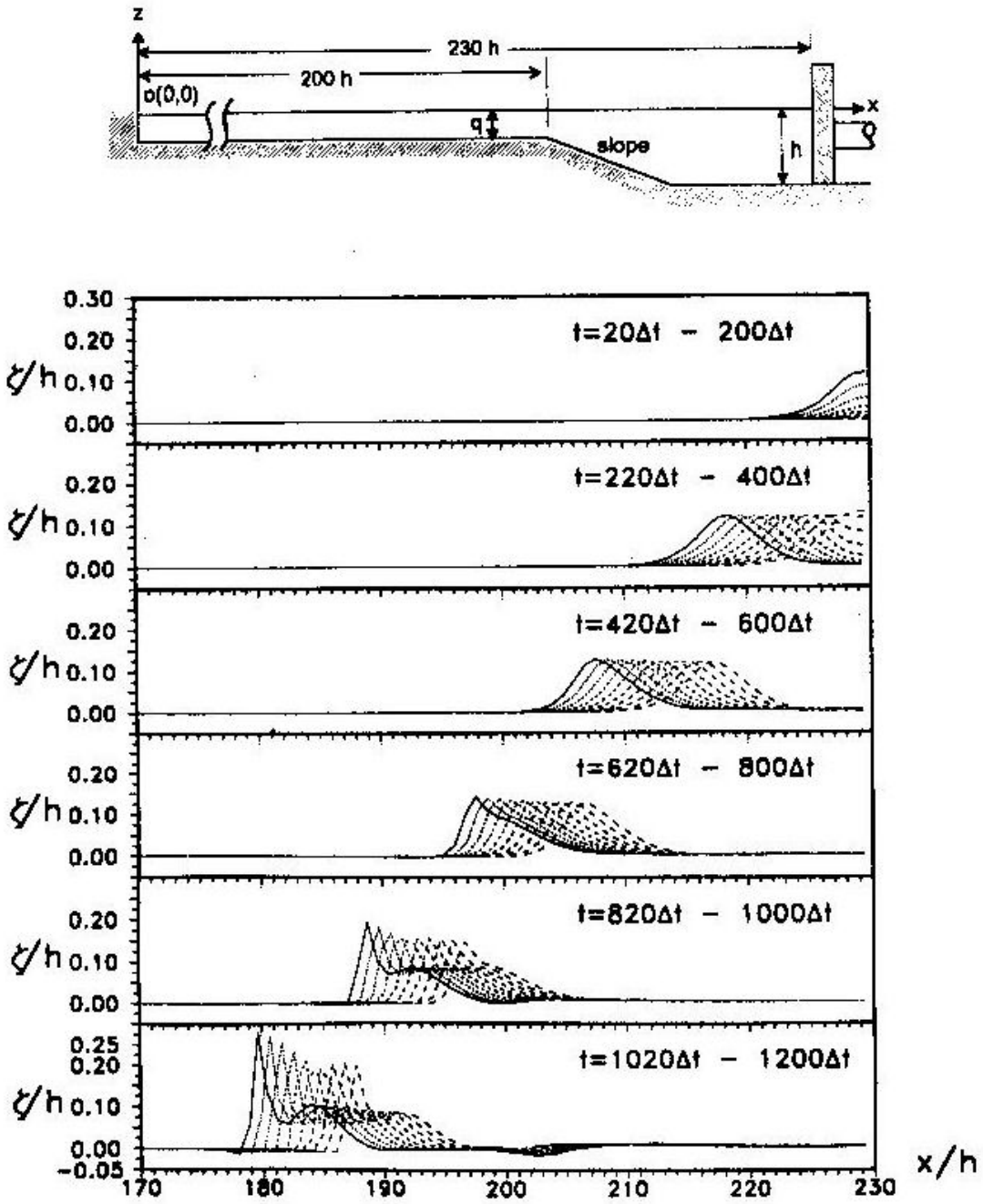

Fig. 8. Deformation of a solitary wave propagating over a slope onto a shelf. $\xi_0/h = 0.12$, $t_c = 3.1593$, $\Delta t = t_c/200$, $q/s = 0.5$, slope = 1:30.

5. Conclusions

The algorithm in this research with the boundary element technique based on the Lagrangian description and finite differential method to time is applied to analyze the problems of generation and deformation of solitary waves. It is found that the numerical instability of the present scheme will be present for slopes greater than 1:5 in the absence of a shelf, in the presence of a shelf, the stability is good when the water depth on the shelf is large, e. g., larger than 0.5 h. However, the results of the generation and deformation of waves indicate favorable agreement.

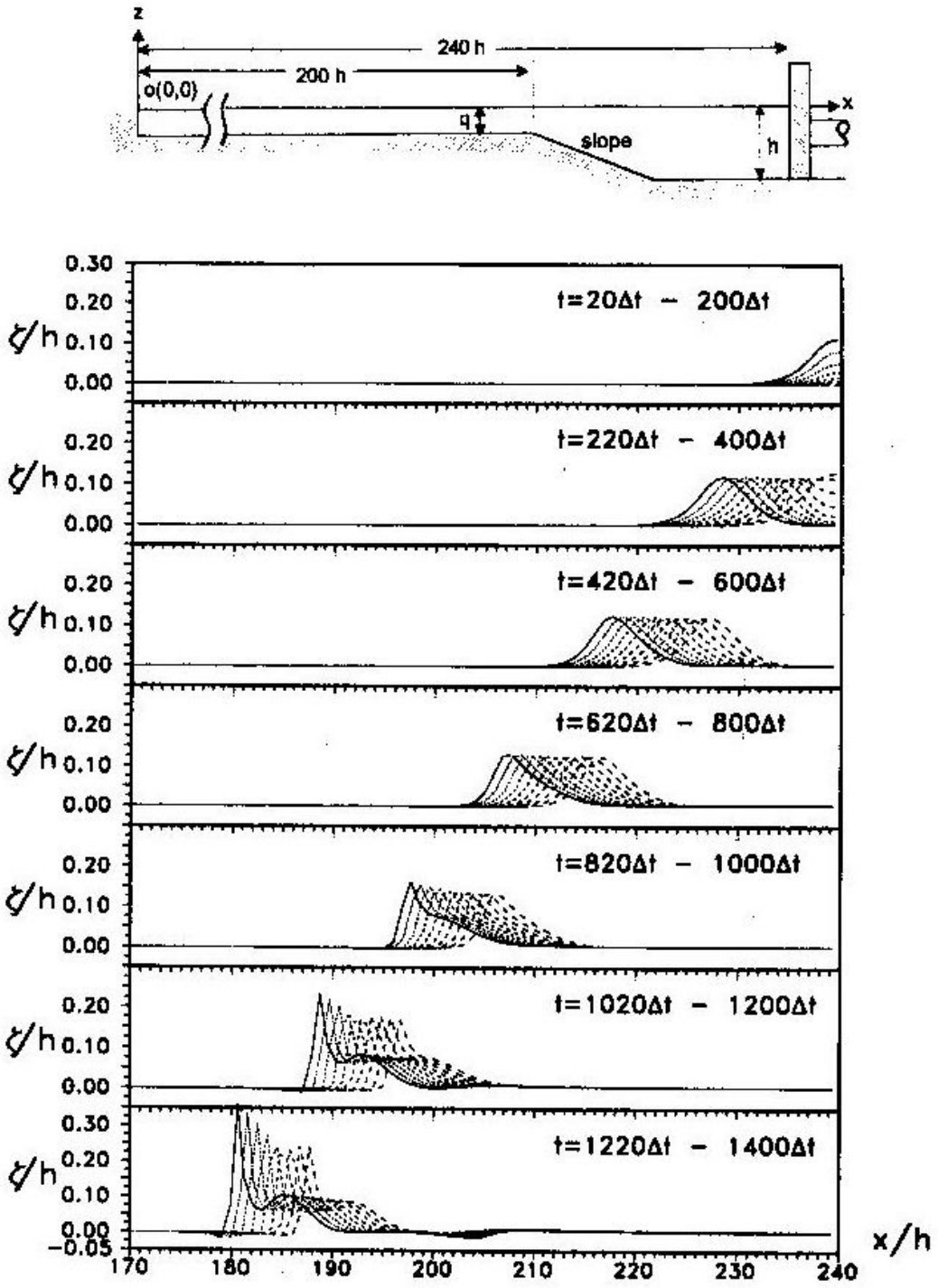

Fig. 9. Deformation of a solitary wave propagating over a slope onto a shelf. $\xi_0 / h = 0.12$, $t_c = 3.1593$, $\Delta t = t_c / 200$, $q / s = 6.5$, slope = 1:20.

Acknowledgements — This research is sponsored by the National Science Council under the Grant NSC-84-2611-E-0190-006. The advice and financial support of the council are gratefully acknowledged.

References

Chou, C. R., 1983. *The Application of Boundary Element Method to Water Wave Mechanics*. National Taiwan College of Marine Science and Technology, Harbor and Ocean Eng. Press, Keelung, China. (in Chinese).

Chou, C. R., Shih, R. S. and Fang, H. M., 1996. Deformation of solitary wave in coastal zones, *Proc. of the 7th Japan-China Symposium on Boundary Element Method*, Elsevier Press, 171~180.

Johnson, R. S., 1972. Some numerical solutions of a variable-coefficient Korteweg-de Vries equation (with applications to solitary wave development on a shelf), *J. Fluid Mech.*, **54**, 81~91.

Madsen, O. S. and Mei, C. C., 1969. The transformation of a solitary wave over an uneven bottom, *J. Fluid Mech.*, **39**, 781~791.

Nakayama, T., 1983. Boundary element analysis of nonlinear water wave problems, *International journal for numerical method in Engineering*, 19, 953~970.

Okamura, K. and Yakuwa, I., 1987. Explicit solution of nonlinear solitary waves propagating over an uneven bottom using the BEM and Lagrange-particle method, *Japan / Boundary Element Symposium*, 233~238. (in Japanese)

Ouyama, Isao., 1985. Boundary element analysis of wave forces due to the reflection of nonlinear solitary waves, *Proc. 33rd Conf. Coastal Engineering*, 555~559. (in Japanses)

Sugino, R. and Tosaka, N., 1990. Boundary element analysis of nonlinear water wave problems, *Pacific Congress on Marine Science and Technology*, 18~25.